



SEISMIC PERFORMANCE ON RC AND PRECAST CONCRETE COLUMNS USING ULTRA HIGH STRENGTH MATERIALS SUBJECTED TO VARYING AXIAL LOAD

T. Matsumoto¹, H. Nishihara¹ and M. Nakao²

ABSTRACT

In order to clarify the flexural performance of RC and precast concrete columns with ultra-high-strength materials, a static bending shear force test was conducted. The specimens were manufactured for the combinations of concrete design nominal strength F_c 80 N/mm² and F_c 120 N/mm², nominal yield strength of the longitudinal reinforcements 490 N/mm² and 685 N/mm², and nominal yield strength of shear reinforcement 1275 N/mm². In the experiment, anti-symmetric bending shear force was repeatedly applied to the specimens of exterior columns in the lower stories subjected to varying axial load. The flexural capacity obtained from the experiment was evaluated using the equation of Building Code and Commentary ACI 318, and it was found that the flexural capacity of the F_c 120 N/mm² specimen was not necessarily evaluated to be on the safe side. Therefore, the flexural capacity of each specimen was reevaluated using rectangular stress blocks designed for high-strength concrete.

Introduction

In recent years, reinforced concrete (RC) buildings have become super-high-rise and long-span structures. In such buildings, the columns of the lower stories are subjected to large long-term axial load. Moreover, when an earthquake occurs, a large varying axial load acts on the exterior columns. Therefore, it is necessary to use higher strength concrete and reinforcing bars, and yet the use of more precast (PCa) members to rationalize the construction of such super-high-rise buildings in shorter work periods is also inevitable.

Six specimens, which consist of RC and PCa columns, were manufactured by combining concrete design nominal strength (F_c) 80 N/mm² and 120 N/mm², nominal yield strength of the longitudinal reinforcements 490 N/mm² (SD490) and 685 N/mm² (USD685), and nominal yield strength of shear reinforcement 1275 N/mm² (SBPD1275). This study aimed to clarify the flexural performance of column members made of ultra-high-strength materials by conducting a static bending shear force test on specimens of external columns in the lower stories subjected to varying axial load.

Furthermore, the flexural capacity obtained from the experiment was evaluated to determine whether or not the rectangular stress block method in accordance with the equation of Building Code and Commentary ACI 318-02 (2002), which was designed for normal-strength concrete, is applicable to high-strength concrete such as the specimens used in this study.

¹Technical Research Institute, ANDO Corporation, Fujimino-City, Saitama, 356-0058, JAPAN

²Research Associate, Faculty of Engineering, Yokohama National University, Yokohama-City, Kanagawa, 240-8501, JAPAN

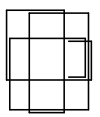
Outline of Experiment

Specimens and Materials

Table 1 shows the structural specifications of each specimen. The six specimens have an area of 330 (width: b) x 330 (overall depth: D) (mm) which is equivalent to 1/3 of the actual column cross-sectional area and a shear span ratio ($M/(V \cdot D)$) of 2.0 in consideration of flexural failure. As shown in Table 1, the specimens are roughly divided into three specimens of F_c 80 N/mm² and another three specimens of F_c 120 N/mm². The values of longitudinal reinforcements 16-D22(# 7) (Grade: SD490) and 16-D19(# 6) (Grade: USD685) for monolithic cast RC column members with respect to each F_c value, and full-PCa column members of the latter value of 16-D19 (USD685) were taken into consideration as the variable factors of the specimens. Four of the 16 longitudinal reinforcements are core reinforcing bars for use in exterior columns in the lower stories. The lateral ties (hoops), used commonly in all the specimens, were small-diameter deformed PC steel bars arranged in a single-stroke enclosed lattice pattern.

The specimens 'C80D22' and 'C80D19' shown in Table 1 have different ratios of total area of longitudinal reinforcements to the gross area of column concrete cross-section (A_{st}/A_g) but their calculated flexural strengths are almost the same. On the other hand, the specimen 'PC80D19' uses a mortar-filled splice sleeve joint to join the longitudinal reinforcements in both column base and capital. The hoops used in these joint sections are the same as those used in other sections. The specimens 'C120D22', 'C120D19', and 'PC120D19' have the same structural specifications as the specimens 'C80D22', 'C80D19', and 'PC80D19' respectively, except for their F_c being 120 N/mm². Fig. 1 shows the shapes of specimens and their bar arrangement.

Table 1. Structural specifications of test specimens.

Specimen	Longitudinal reinforcement A_{st}/A_g (%)	Concrete F_c (N/mm ²)	Hoop (PC steel bar) p_h (%)	Varying axial load P
C80D22	16-D22(SD490) 5.69%	F_c 80		Compressive: +0.55 $F_c bD$ (+0.50 $F_c bD$)* Tensile: -0.7 $A_{st} f_y$
C80D19	16-D19(USD685)			
PC80D19	4.22%			
C120D22	16-D22(SD490) 5.69%	F_c 120	4-RB6.2 @50 (SBPD 1275/1420) 0.73%	
C120D19	16-D19(USD685)			
PC120D19	4.22%			

*0.50 $F_c bD$ in the case of F_c 120 N/mm².

b (width)=330mm
 D (overall depth)=330mm
 h (clear height)=1320mm
 $M/(VD)$ (shear span ratio)=2.0

Table 2. Mechanical properties of reinforcements.

Bar size	f_y N/mm ²	ϵ_y	f_t N/mm ²	E_s kN/mm ²	Elongation %
D22(#7)(SD490)	522	0.0028	715	196	17
D19(#6)(USD685)	745	0.0057	1008	202	12
Hoop: RB6.2(#2) (SBPD1275/1420)	1275*	0.0077	1442	198	7

*Taken as the 0.2% proof stress.

f_y = yield strength

ϵ_y = yield strain

f_t = tensile strength

E_s = elastic modulus

Table 3. Mechanical properties of concrete and mortar.

Specimen	f_c' N/mm ²	E_c kN/mm ²	$c f_t$ N/mm ²	Specimen	f_c' N/mm ²	E_c kN/mm ²	$c f_t$ N/mm ²
C80D22	92.4	37.4	5.95	C120D22	135.6	44.3	7.44
C80D19	98.4	38.7	5.48	C120D19	136.0	44.3	6.91
PC80D19	98.7	39.4	5.00	PC120D19	134.4	44.3	6.80
J. mortar*	136.6	41.4	-	J. mortar*	147.8	43.6	-

*Joint mortar and grout.

f_c' = concrete cylinder
compressive strength

E_c = elastic modulus

$c f_t$ = splitting strength

Table 2 shows the mechanical properties of the reinforcements used in this experiment. Table 3 shows the mechanical properties of the concrete. The concrete materials for the specimens include high-early-strength Portland cement for F_c 80 N/mm² and normal Portland cement for F_c 120 N/mm² with about 10 WT% of silica fume as admixture. Crushed stones having the maximum diameter of 13 mm were used as coarse aggregate for all the specimens.

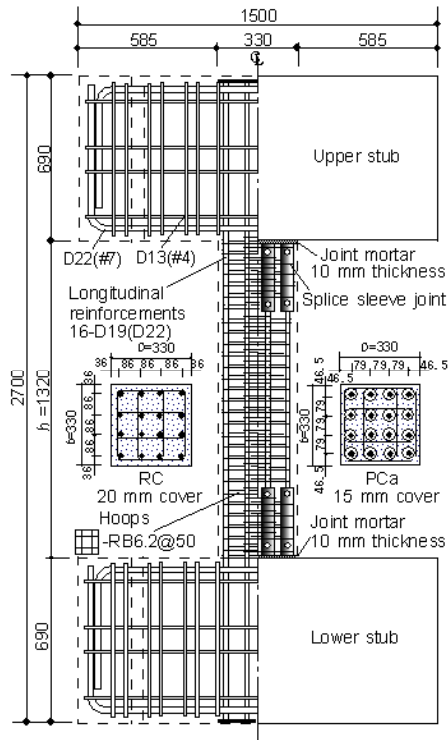


Figure 1. Dimensions of specimens.
(All dimensions in mm)

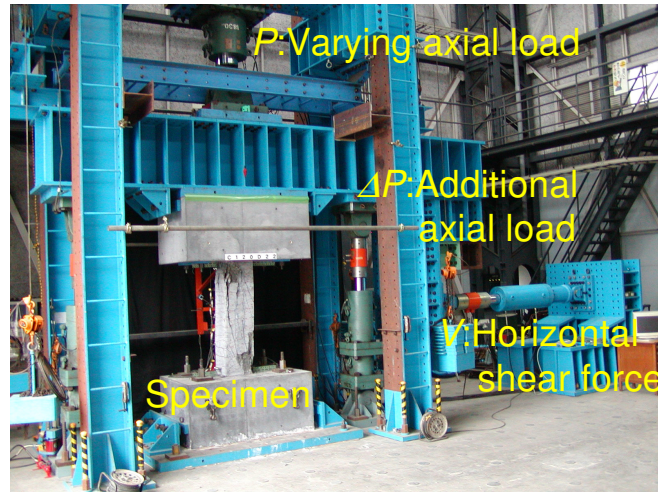


Photo 1. Loading conditions.

Loading Methods

For loading specimens, an L-shaped loading beam as shown in Fig. 2 was used. While varying axial load was applied to the specimen, anti-symmetric static bending shear force, with the center level of the height of the test section being the point of contraflexure, was also applied to the specimen repeatedly, with positive and negative horizontal shear forces applied alternately. Fig. 3 shows the loading method of varying axial load, where the compressive axial load is expressed as positive load. First, long-term compressive axial load of $0.2F_c bD$ was applied. Then, axial load (P) was gradually changed in accordance with the horizontal shear force (V). The upper limit and lower limit of the axial load were the compressive axial load $0.55F_c bD$ ($0.50F_c bD$ in the case of F_c 120 N/mm²) in positive shear force loading and the tensile axial load $-0.7A_{st} f_y$ ($A_{st} f_y$: product of the total area of the longitudinal reinforcements and the actual yield strength) in negative shear force loading. The axial load was kept constant thereafter.

The horizontal shear force was controlled on the basis of story drift angle ($R = \delta/h$, δ : relative horizontal displacement between upper and lower stubs, h : clear height of column). The experiment was terminated after applying shear force once at $R = \pm 2.5/1000$, twice at $R = \pm 5/1000$, $\pm 10/1000$, $\pm 15/1000$, and $\pm 20/1000$, and once at $R = \pm 30/1000$ and $\pm 50/1000$ respectively. Photo 1 shows the loading conditions.

Results of Experiment

Outline of the Results

Fig. 4 shows the relationship between the shear force (V) and story drift angle (R) of all specimens with $P-\Delta$ effect taken into consideration. The single-dot chained lines in the Fig. 4 represent the proof strength in the case where the hysteretic curve with $P-\Delta$ effect taken into consideration is lowered to a level that is 95% of the maximum shear force. Table 4 shows the shear strength and story drift angle of each loading. The shear strength values in the Table 4 are those with $P-\Delta$ effect taken into consideration, except for the “first cracking”. Photo 2 shows the final conditions ($R = +50/1000$) of the specimens.

Process of Crack and Failure

The first cracking in each specimen was not detected while applying positive shear force in the first cycle. However, cracking started at the joint ends between the test section and the upper and lower stubs immediately after starting to apply tensile axial load in negative shear force mode. After that, flexural tensile cracking was detected, scattered throughout almost the entire test section. Although slightly fewer tensile cracks were generated in PCa column specimens ‘PC80D19’ and ‘PC120D19’ than in the other specimens, no influence of joint mortar sections was observed.

The specimens ‘C80D22’ and ‘C120D22’ that employed SD490 for the longitudinal reinforcements had compressive yield in their longitudinal reinforcements at about $R = +5/1000$, then the cover concrete immediately started to spall. As for the specimens ‘C80D19’, ‘PC80D19’, ‘PC120D19’, and ‘PC120D19’, which employed USD685 for the longitudinal reinforcements, spalling preceded in the concrete at $R = +5/1000$ through $+10/1000$, and compressive yield occurred in their longitudinal reinforcements at about $R = +10/1000$. In particular, the shear strength when PCa column specimens ‘PC80D19’ and ‘PC120D19’ spalled at $R = +5/1000$ through $+10/1000$ reached almost the maximum shear strength; the hysteretic characteristics thereafter might have been affected.

Table 4. Experimental results of specimens.

Specimen	f_c' N/mm ²	\pm	V_{cr} kN	R_{cr} x1/1000	V_y kN	R_y x1/1000	V_{co} kN	R_{co} x1/1000	V_{max} kN	R_{max} x1/1000	V_{ul} kN
C80D22	92.4	+	—	—	755.5	5.47	774.7	5.92	948.9	20.05	909.5
		-	-51.9	-0.73	-75.4	-4.58	—	—	-325.4	-30.02	-325.4
C80D19	98.4	+	—	—	786.2	9.99	770.3	6.48	938.8	20.02	900.5
		-	-37.9	-0.48	-159.3	-9.70	—	—	-347.4	-29.64	-347.4
PC80D19	98.7	+	—	—	838.6	10.93	870.5	7.61	935.1	29.26	873.4
		-	-37.9	-0.50	-148.0	-9.42	—	—	-360.9	-29.33	-360.9
C120D22	135.6	+	—	—	877.7	4.78	888.0	5.00	1022.7	15.03	849.5
		-	-54.9	-0.58	-89.8	-5.02	—	—	-326.2	-28.37	-326.2
C120D19	136.0	+	—	—	972.5	12.08	892.0	6.08	1013.4	15.01	912.1
		-	-56.9	-0.61	-188.2	-12.74	—	—	-353.2	-30.02	-353.2
PC120D19	134.4	+	—	—	897.1	7.96	955.1	6.73	968.8	10.02	881.1
		-	-53.9	-0.45	-123.3	-7.60	—	—	-385.2	-30.04	-385.2

f_c' = concrete cylinder compressive strength

V_{cr} (R_{cr}) = shear strength (drift angle) at the first cracking

V_y (R_y) = shear strength (drift angle) at the yield of longitudinal reinforcement

V_{co} (R_{co}) = shear strength (drift angle) at the spalling of cover concrete (1st peak)

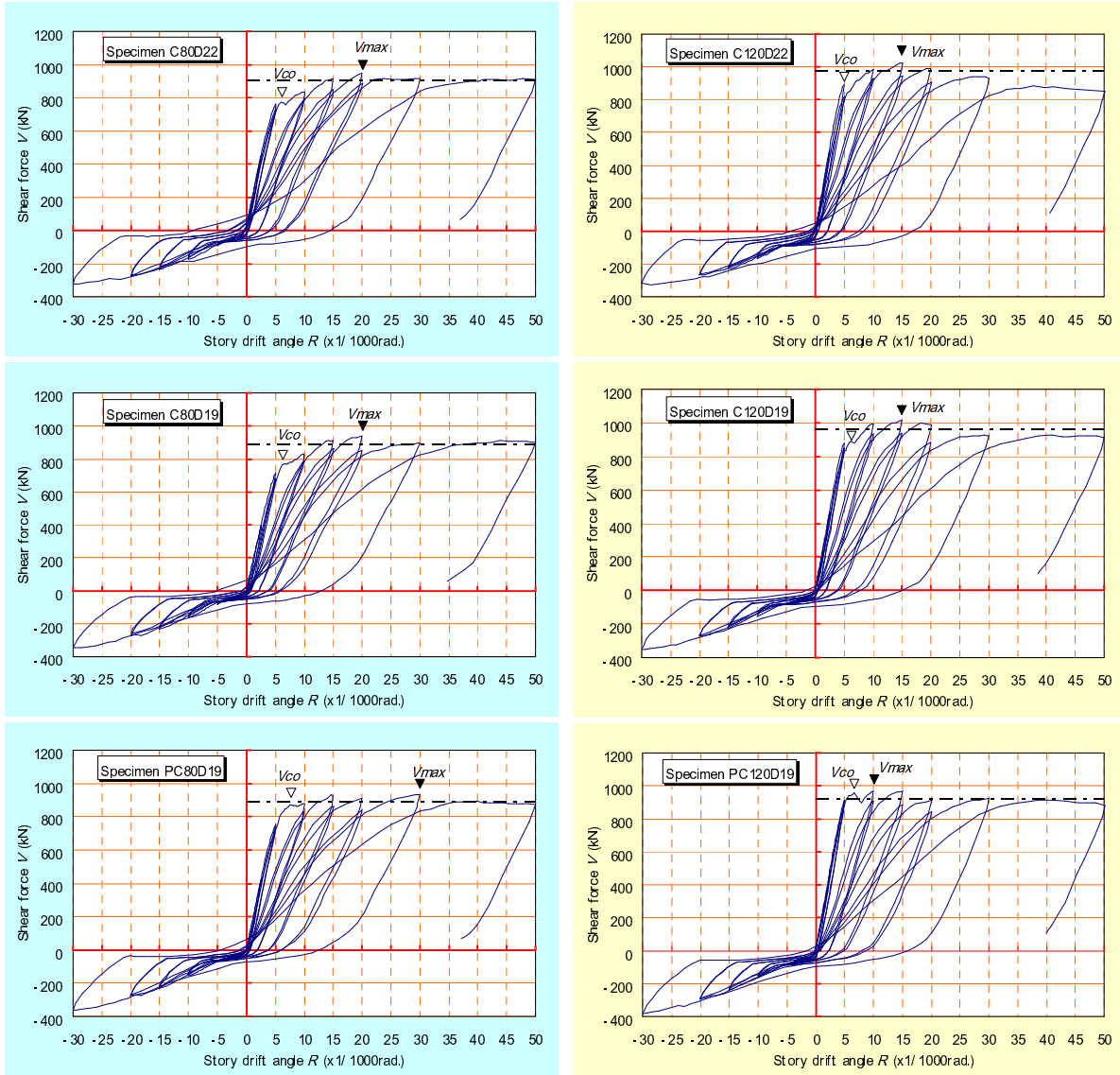


Figure 4. Relationship between the shear force (V) and story drift angle (R).

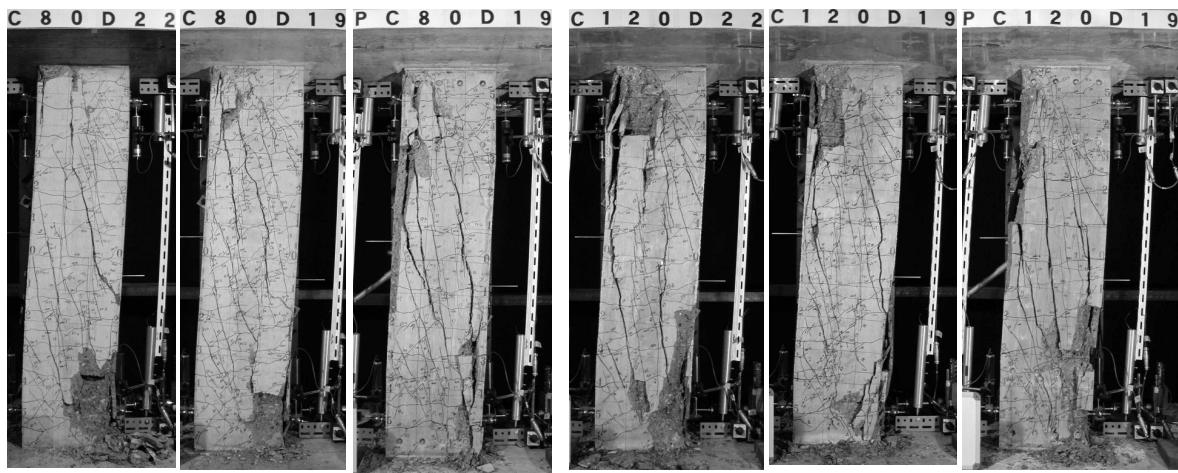


Photo 2. Final conditions ($R = +50/1000$) of specimens.

A number of cracks, which were different from bonding splits, in the vertical direction at the center position of the test section were observed at $R = +10/1000$. In the case of PCa column specimens, those cracks expanded diagonally from the lower joint end of the column capital to the upper joint end of the column base. When maximum shear force with $P-\Delta$ effect taken into consideration was applied, both specimens 'C80D22' and 'C80D19' were at $R = +20/1000$ and the specimen 'PC80D19' was at $R = +30/1000$. Furthermore, while the specimens 'C120D22' and 'C120D19' were at $R = +15/1000$, the specimen 'PC120D19' was at $R = +10/1000$. However, a drop in shear strength at $R = +15/1000$ was hardly observed. With all the specimens, the negative shear force kept increasing up to about $R = -30/1000$ during tensile axial load.

The failure patterns shown in Photo 2 show flexural crushing in the column capital and column base of the specimens. With the PCa column specimens 'PC80D19' and 'PC120D19', the degree of shear cracking in the central area of the test section and crushing from the joints to the positions just above the joints was remarkable. However, no such phenomena as buckled longitudinal reinforcements and rupture of hoops were observed in any specimen.

Strains in Axial Direction

Fig. 5 shows the relationship between the axial strain and story drift angle of each specimen. For the expression of the axial strains, the elongation displacement between upper and lower stubs at the axial position in the column was divided by the clear height of column (h) and the tensile strain was expressed as a positive value. The strain performance in the axial direction of the $F_c 80 \text{ N/mm}^2$ and $F_c 120 \text{ N/mm}^2$ specimens while applying tensile axial load remained almost the same. The axial strains of the $F_c 120 \text{ N/mm}^2$ specimen during the large deformation period at and after $R = +10/1000$ in compressive axial load application mode became large. Also from the appearance of final condition shown in Photo 2, it is clear that the degree of crushing in the $F_c 120 \text{ N/mm}^2$ specimen is larger than that in the $F_c 80 \text{ N/mm}^2$ specimen, together with spalling of cover concrete over a larger surface area of the $F_c 120 \text{ N/mm}^2$ specimen. According to the equation of Building Code and Commentary ACI 318-02 (2002), the axial compressive capacity of a column member using normal-strength concrete is given by the following equation:

$$P_0 = 0.85 f_c' (A_g - A_{st}) + A_{st} f_y \quad (1)$$

In connection with Eq. 1 above, Ozbakkaloglu and Saatcioglu (2004) proposed the following equation as an axial compressive capacity expression applicable to a column using concrete of strengths from normal to high-strength level (120 N/mm^2).

$$P_{0(HSC)} = 0.9 k_4 f_c' (A_g - A_{st}) + A_{st} f_y \quad (2)$$

$$k_4 = \gamma + (1 - \gamma) A_c / A_g \leq 0.95 \quad (3)$$

$$\gamma = 1.1 - 0.007 f_c' \leq 0.8 \quad (4)$$

Table 5 shows the axial compressive capacity of each specimen obtained by using Eqs. 1 and 2. The rate of loaded axial force, which is obtained by dividing the compressive axial load (P) applied to each specimen by the product of the compressive strength of concrete (f_c') and total cross-sectional area of the column (A_g), is slightly larger in the $F_c 80 \text{ N/mm}^2$ specimen than in the $F_c 120 \text{ N/mm}^2$ specimen. However, calculation of the ratios of axial compressive capacity (P_0), based on Eqs. 1 and 2, to the loaded axial force (P) resulted in a clearly greater ratio for the $F_c 120 \text{ N/mm}^2$ specimen in Eq. 2 than in Eq. 1 of ACI 318-02 (2002). It is safe to assume that this greater ratio caused the increase in the axial strains of the $F_c 120 \text{ N/mm}^2$ specimen during the large story drift angle. There was no difference in the axial strains between RC column specimens prepared by monolithic casting and PCa column specimens.

Evaluation of Flexural Capacity

To identify the deformation component of each specimen, the test section was divided into four sub-sections in increments of $1.0 D$. The flexural deformation and shear deformation in each sub-section were studied, with the result that flexural deformation is about 70% of the total deformation. Then, the experimental shear strength values for spalling of cover concrete and maximum horizontal force (referred to also as “first peak: V_{co} ” and “second peak: V_{max} ”) shown in Table 4 were compared with calculated values respective-ly, as shown in Table 6.

The calculated values, with respect to the coefficients (α_1 and β_1) which constitute the rectangular stress block as shown in Fig. 6, were based on both (i) Equation of Building Code and Commentary ACI 318-02 (2002) and (ii) Equation proposed by Ozbakkaloglu and Saatcioglu (2004). The coefficients α_1 and β_1 represented by both (i) and (ii) at a compressive strength of concrete $f'_c \geq 30 \text{ N/mm}^2$ are shown below. The ultimate compressive strain at extreme fiber (ϵ_u) is 0.003 in common.

(i) Equation of Building Code and Commentary ACI 318-02 (2002)

$$\alpha_1 = 0.85 \tag{5}$$

$$\beta_1 = 0.85 - 0.008 (f'_c - 30) \geq 0.65 \tag{6}$$

(ii) Equation proposed by Ozbakkaloglu and Saatcioglu (2004)

$$\alpha_1 = 0.85 - 0.0014 (f'_c - 30) \geq 0.72 \tag{7}$$

$$\beta_1 = 0.85 - 0.0020 (f'_c - 30) \geq 0.67 \tag{8}$$

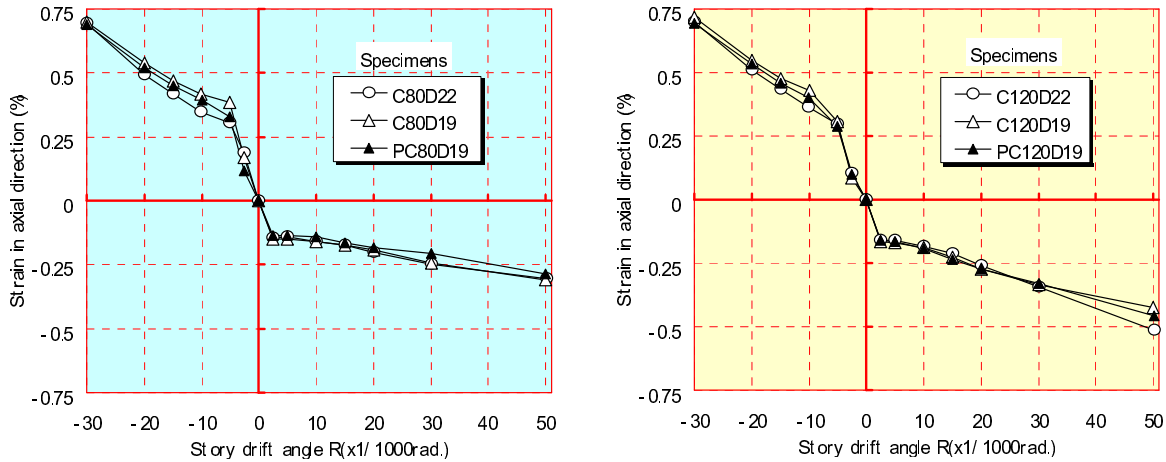


Figure 5. Relationship between the strain in the axial direction and story drift angle.

Table 5. Axial compressive capacity of specimens.

Specimen	f'_c N/mm ²	A_g mm ²	A_c mm ²	A_{st} mm ²	P kN	$P/(f'_c A_g)$	P_0 kN	P/P_0	mean	$P_{0(HSC)}$ kN	$P/P_{0(HSC)}$	mean
C80D22	92.4		80656	6192		0.477	11299	0.425		10562	0.454	
C80D19	98.4	108900	80656	4592	4800	0.448	12145	0.395	0.405	11248	0.427	0.442
PC80D19	98.7		71824	4592		0.447	12172	0.394		10823	0.444	
C120D22	135.6		80656	6192		0.440	15070	0.431		13006	0.500	
C120D19	136.0	108900	80656	4592	6500	0.439	15479	0.420	0.425	13367	0.486	0.503
PC120D19	134.4		71824	4592		0.444	15337	0.424		12426	0.523	

P = upper limit of the compressive axial load

P_0 = nominal concentric compressive capacity, defined in Eq. 1

$P_{0(HSC)}$ = nominal concentric compressive capacity, defined in Eq. 2

The experimental shear strength values of both the first and second peak were evaluated with respect to the case where $P-\Delta$ effect was taken into consideration as well as the case where $P-\Delta$ effect was not taken into consideration.

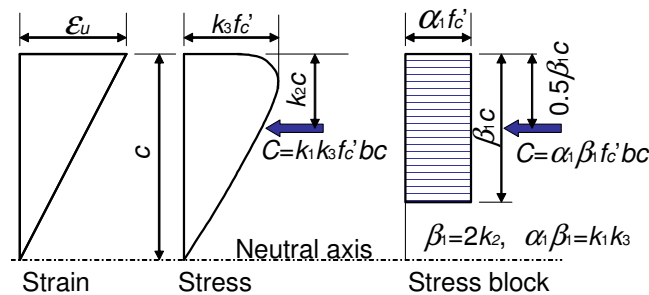


Figure 6. Rectangular stress block.

According to Table 6, the experimental shear strength values of both the first and second peak of $F_c 80$ N/mm^2 specimens are higher than the calculated values determined by Eqs. (i) and (ii) even in the case where $P-\Delta$ effect is not taken into consideration. Because the calculated shear strength values determined by Eqs. (i) and (ii) were based on the assumption that ϵ_u is 0.003 equally, the shear strength from the first peak, or spalling of the cover concrete, seems to have been included. Table 6 also indicates that the calculated values of the specimens 'C80D22' and 'C80D19' are almost equal to the experimental values of shear strength during the first peak. The experimental shear strength values rose thereafter, too. This means that the second peak, or the shear strength under the maximum load, has a safety factor that is about 1.2 times the values calculated from Eqs. (i) and (ii), even in the case where $P-\Delta$ effect is not taken into consideration and that the equations can be employed in the structural design.

Regarding the $F_c 120$ N/mm^2 specimens, the experimental shear strength values during the first and second peak, on the basis of the values calculated by Eq. (i) of Building Code and Commentary ACI 318-02 (2002), cannot be evaluated to be on the safe side. In Eq. (ii) proposed by Ozbakkaloglu and Saatcioglu (2004), the coefficients α_1 and β_1 of the Eq. (i) are modified so that the equation can be applied to concrete columns of strengths from normal to high-strength. Using this Eq. (ii), the experimental shear strength values during the first and second peak of $F_c 120$ N/mm^2 specimens can be evaluated to be nearly on the safe side. However, the safety factor of the experimental shear strength values for $F_c 120$ N/mm^2 specimens during the second peak is comparatively low with respect to that of $F_c 80$ N/mm^2 specimens.

It is assumed that the ultimate compressive strain at extreme fiber (ϵ_u) is 0.003 in the flexural capacity calculation method using these rectangular stress blocks. This is the reason why it is not suitable for calculating the shear strength during the second peak (flexural capacity) where the high-strength longitudinal reinforcements of a column undergo compressive yield phenomenon as observed in this study.

Table 6. Comparison of experimental and calculated flexural capacity values.

Specimen	<i>P-Δ</i> effect	<i>V_{co}</i> kN	<i>V_{max}</i> kN	<i>V_{ACI}</i> kN	1st		<i>V_{HSC}</i> kN	2nd	
					<i>V_{co}/V_{ACI}</i>	<i>V_{max}/V_{ACI}</i>		<i>V_{co}/V_{HSC}</i>	<i>V_{max}/V_{HSC}</i>
C80D22	no	746.3	853.1	726.8	1.03	1.17	727.4	1.03	1.17
	yes	774.7	948.9		1.07	1.31		1.07	1.30
C80D19	no	739.3	843.1	720.5	1.03	1.17	704.4	1.05	1.20
	yes	770.3	938.8		1.07	1.30		1.09	1.33
PC80D19	no	834.1	857.1	697.2	1.20	1.23	680.6	1.23	1.26
	yes	870.5	935.1		1.25	1.34		1.28	1.37
C120D22	no	855.3	924.8	968.6	0.88	0.95	858.8	1.00	1.08
	yes	888.0	1022.7		0.92	1.06		1.03	1.19
C120D19	no	852.4	929.6	930.5	0.92	1.00	819.6	1.04	1.13
	yes	892.0	1013.4		0.96	1.09		1.09	1.24
PC120D19	no	911.1	903.7	896.9	1.02	1.01	788.2	1.16	1.15
	yes	955.1	968.8		1.06	1.08		1.21	1.23

V_{ACI} = flexural capacity calculated by Equation of ACI 318-02 (2002)

V_{HSC} = flexural capacity calculated by Equation of Ozbakkaloglu and Saatcioglu (2004)

Conclusions

A bending shear force test was conducted on RC and precast concrete columns with ultra-high-strength materials subjected to varying axial force, and the following findings were obtained. We have to design RC and precast concrete columns while taking account of the following conclusions in the future.

1. With almost equal calculated flexural strength provided for specimens with longitudinal reinforcements D22(# 7) (SD490) and D19(# 6) (USD685), the former developed spalling of cover concrete immediately after the compressive yield of longitudinal reinforcements, while the latter first developed spalling of cover concrete and then compressive yield of longitudinal reinforcements.

2. Specimens with a concrete design nominal strength of F_c 80 N/mm² and F_c 120 N/mm² were subjected to a load of compressive axial force of $0.55F_c bD$ and $0.50F_c bD$ respectively. The axial strains during large story drift angle in the F_c 120 N/mm² specimen was larger than that in the F_c 80 N/mm² specimen, while spalling of cover concrete developed widely in the F_c 120 N/mm² specimen.

3. PCa column specimens of both F_c 80 N/mm² and F_c 120 N/mm² indicated larger shear strength during cover concrete spalling than RC column specimens. On the contrary, an increase in shear strength thereafter was small. The maximum shear strength of PCa column specimens was also a little lower than that of the RC column specimens prepared by monolithic casting.

4. The flexural capacity of each specimen was evaluated by the rectangular stress block method in compliance with Building Code and Commentary ACI 318-02 (2002). The flexural capacity levels obtained with F_c 80 N/mm² specimens were largely on the safe side, whereas those obtained with F_c 120 N/mm² were not necessarily on the safe side. However, it was confirmed that the experimental values were considered to be on the safe side by applying the stress blocks in accordance with the proposal of Ozbakkaloglu and Saatcioglu (2004) to the evaluation.

Notation

- A_c = area of core concrete within perimeter hoop (center-to-cente)
 A_g = gross area of column cross-section
 A_{st} = total area of longitudinal reinforcement
 b = width of a column cross-section

- D = overall depth of a column cross-section
 F_c = design nominal strength of concrete
 f'_c = concrete cylinder compressive strength
 f_y = yield strength of longitudinal reinforcement
 P = axial load
 P_0 = nominal concentric compressive capacity of a column calculated according to Eq. (1)
 $P_{0(\text{HSC})}$ = nominal concentric compressive capacity of a column using concrete of strength from normal to high-strength level (120 N/mm^2) calculated according to Eq. (2)
 α_1 = coefficient that defines width of rectangular stress block specified in Fig. 6
 β_1 = coefficient that defines height of rectangular stress block specified in Fig. 6
 ϵ_u = extreme compression fiber strain in concrete at ultimate moment resistance
 γ = coefficient defined in Eq. (4)

References

- ACI Committee 318, 2002. *Building Code Requirement for Structural Concrete (ACI 318-02) and Commentary (318R-02)*, American Concrete Institute, Farmington Hills, Mich.
- Ozbakkaloglu, T., and Saatcioglu, M., 2004. Rectangular Stress Block for High-Strength Concrete, *ACI Structural Journal* 101(4), 475-483.